An ensemble-based method to assess the quality of a sample of nanocrystals as single photon emitters

Stefano Vezzoli [a,b,*], Seyedruhollah Shojaii [a], Simone Cialdi [a,c], Daniele Cipriani [a], Fabrizio Castelli [a,c], Matteo G.A. Paris [a,d], Luigi Carbone [e], P. Davide Cozzoli [e,f], Elisabeth Giacobino [b], Alberto Bramati [b]

[a] Università degli Studi di Milano, Dipartimento di Fisica, Via Celoria 16, 20133 Milan, Italy
[b] Université Pierre et Marie Curie, Laboratoire Kastler Brossel, CNRS UMR8552, Ecole Normale Supérieure, 4 place Jussieu, 75252 Paris Cedex 05, France
[c] INFN, Sezione di Milano, Via Celoria 16, I-20133 Milan, Italy
[d] CNISM, Udr Milano, I-20133 Milan, Italy
[e] National Nanotechnology Laboratory - Istituto Nanoscienze CNR, Via Arnesano 16 – 73100 Lecce, Italy
[f] Dipartimento di Matematica e Fisica "E. De Giorgi" – Università del Salento, Via Arnesano 73100 Lecce, Italy

ARTICLE INFO

ABSTRACT

Colloidal semiconductor nanocrystals are among the best candidates for realizing a nano-structured single photon source at room temperature. In this paper we present a new and efficient optical method to assess the quality of a sample of nanocrystals as single-photon emitters, by an ensemble measurement of photoluminescence. We relate the ensemble photoluminescence measurements to the photon statistics of single emitters by a simple theoretical model. As an example we compare two different kinds of CdSe/CdS dot-in-rods, showing a similar degree of single photon emission when observed on a selection of single nanocrystals. The results are compared with anti-bunching measurements realized on single nanocrystals of the two kinds.

Since the first experiments in the 1990s [1–3], colloidal semiconductor nanocrystals (NCs) have been intensively studied for their optical properties due to quantum confinement. In particular they were demonstrated to be good potential single photon sources at room temperature [4]. Many strategies have been pursued in order to improve their single photon source performances, such as embedding NCs in photonic nano-structures, or tuning their shape and material composition [5]. Multiphoton emission suppression is assigned to an enhanced Coulomb interaction between excitons that gives rise to the so called non-radiative Auger recombination [6], in which an exciton recombines while transferring its energy to another exciton. On the other hand, Auger processes are also usually invoked to explain one of the main physical drawbacks of NCs, namely blinking [7,8]. This is a reversible photo-luminescence (PL) bleaching which is usually associated with ionization [9], and which has been observed also in other quantum systems like single molecules [10]. Because of Auger effect, absorbed energy can be efficiently transferred from one electron–hole pair to a third charge. This spectator charge can be already trapped in some defects or it can be ejected from the confinement potential as a consequence of photo-excitation. When a NC is ionized, it is either in a non-emissive *off* state [8] or in a low emitting *gray* state [11]. In addition, a permanent (i.e. much longer than the experimental time scale) PL bleaching can be caused either by multiple ionization events or by intrinsic photo-chemical instability. In fact, NCs can also enter a low emitting state because of non-radiative processes other than Auger, such as phonon relaxation or energy transfer to trap states. The resistance of NCs to such photo-induced degradation processes is usually referred as photo-stability.

Photo-stability and blinking are naturally interconnected. They both originate from strong quantum confinement, on one side, and from the interactions of the nano-structure with the environment through its large surface, on the other side. Effective passivation can be provided both by growing an inorganic shell of suitable material [12] and surrounding the NCs with organic ligands. Suppression of blinking was obtained in colloidal systems like graded alloy core–shell CdZnSe/ZnSe [13] or quantum dot-quantum rod structures [14,15]. A suppression of Auger recombination, together with a high photo-stability, has been demonstrated in giant shell CdSe/CdS NCs [16,17]. However, this improvement in PL stability has lead to a drawback: non-blinking NCs, such as self-assembled quantum dots, are usually no longer good single photon emitters [18]. In order to reach a good trade-off between preserving single photon emission and

* Corresponding author at: Université Pierre et Marie Curie, Laboratoire Kastler Brossel, CNRS UMR8552, Ecole Normale Supérieure, 4 place Jussieu, 75252 Paris Cedex 05, France. Tel: +33 01 44 27 43 19.
E-mail address: stefano.vezzoli@unimi.it (S. Vezzoli).

reaching good photo-stability, many strategies can be pursued: tuning dimension, shape and material of the shell, selecting suitable coordinating ligands [20,21], applying electrochemical potential or choosing a suitable substrate in order to control NCs state of charge [9,19]. All these parameters can be a source of great variability in quantum properties, even within a same sample of NCs.

Photo-stability can be assessed by ensemble measurements, for example by exposing the NCs solution to UV light and by observing the PL spectrum. However, these kinds of tests do not give any information about quantum optical properties. On the other hand, measurements on single isolated NCs, which are usually required to assess photon statistics, may not be statistically significant for quantifying the photo-stability of the ensemble. In fact, this kind of measurements usually relies on a pre-selection of bright and photo-stable NCs.

For this reason, a fast and efficient method allowing to evaluate both the photo-stability and the overall single photon source quality of a sample of NCs is expected to be very useful. Such a method would allow, for instance, a fast discrimination between different passivation techniques, or states of conservation, or between two different synthesis of the same kind of NCs.

In this work we describe an ensemble-based method to evaluate the homogeneity of a sample in terms of its photon statistics and its photo-stability. The method consists in measuring the PL of an ensemble of NCs and studying its dependence versus the excitation intensity, under various external conditions, in particular after the NCs have been submitted to irradiation by a high power laser. This allows to select a sample in which most of the NCs are good single-photon sources from another one in which this property is much more dispersed, avoiding long measures on single emitters. It can also test the state of conservation of a sample, or its different reactivity when deposited on different substrates. The ensemble PL measurements have been compared with single photon measurements on a selection of NCs. A model to link single NC properties with ensemble behavior is proposed to interpret the experimental results. In order to show the flexibility of this method, we also study the effect of the interaction with an external atmosphere, which is another critical point for all nanostructures having high surface-to-volume ratio. For example the presence of oxygen can be detrimental for some kind of NCs [22] but it was shown to boost PL for others [23].

We specifically study NCs constituted of a spherical core of CdSe with a cylindrical shell of CdS, a configuration usually referred to as dot-in-rod (DRs), synthesized with a recently developed method [24]. We compare two kinds of DRs, named DR1 and DR2, with different geometrical parameters, summarized in Fig. 1.

First of all anti-bunching measurements on single NCs are performed to investigate their single photon source character. This test is performed on a selection of about 10 NCs which are chosen because they are bright enough to be detected on a CCD camera and because their PL is stable enough to go through an entire session of measurements. Single NCs are excited by a pulsed laser diode at 405 nm (pulse ~50 ps, repetition rate =2.5 MHz) in a confocal configuration and their PL is sent into a Hanbury Brown-Twiss setup. The emission is split into two parts and recorded by two avalanche photodiodes (APD), generating two intensity signals $I_1(t)$ and $I_2(t)$ made of discrete pulses. The coincidences between these counts are measured as a function of the delay τ between the two channels, giving rise to a series of peaks corresponding to laser excitation, as shown in Fig. 2(b). This allows assessing the intensity autocorrelation function:

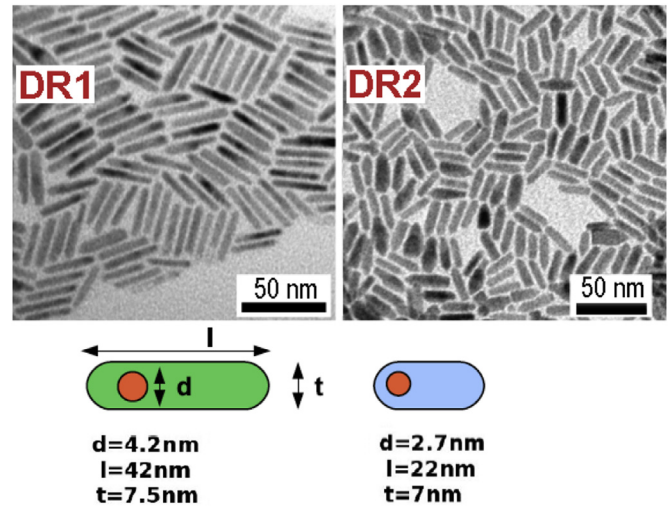$$g^2(\tau) = \frac{\langle I_1(t)I_2(t+\tau)\rangle}{\langle I_1(t)\rangle\langle I_2(t+\tau)\rangle} \qquad (1)$$

Fig. 1. TEM images of the two samples studied in this work, deposited from a toluene solution of density 10^{-8}–10^{-7} M. Geometrical parameters as rod length l and thickness t are estimated from TEM images, whereas core diameter d is that of the CdSe seeds employed for the growth of the elongated CdS shell.

The ratio between the peak in zero and the lateral peaks gives the normalized autocorrelation function at zero delay $\tau = 0$, $g^2(0)$. This is a measure of the single photon source quality. It has been demonstrated that $g^2(0)$, measured at low excitation power, corresponds to the ratio between the probability of two photons and single photon emission [25].

The result of our measurements, depicted in Fig. 2(a), is that both DR1 and DR2 show a good single photon emission for any studied excitation power.

Another method to assess NCs quantum optical properties is to measure single NCs PL as a function of the excitation power. When a laser pulse is absorbed by a NC, it creates N electron–hole pairs (referred to as a N-multiexciton) with a Poissonian distribution $P(N,\langle N\rangle)$, with a mean number $\langle N\rangle$ which is proportional to the excitation power. Any m-multiexciton state decays to the $(m-1)$ state via a electron–hole recombination, with a probability QY_m to emit a photon. This process is repeated until all the electron–hole pairs have recombined. This model [18] gives the following expression for the mean photon number I_{PL} emitted by the nano-crystal:

$$I_{PL}(\langle N\rangle) = \sum_{N=1}^{\infty} P(N,\langle N\rangle) \sum_{m=1}^{N} QY_m \qquad (2)$$

The probability of radiative recombination is equal to the Quantum Yield QY_m:

$$QY_m = \frac{\gamma_{R,m}}{\gamma_{R,m}+\gamma_{A,m}+\gamma_{NR,m}} \qquad (3)$$

where γ_R is the radiative recombination rate, γ_A is the Auger recombination rate, responsible for single photon emission, and γ_{NR} takes into account other non-radiative decay channels different from Auger, like energy transfer to phonons or to surface defects. All these rates scale with the number of charges excited by the laser [9]. Single photon Quantum Yield QY_1 can be as high as 70% in both DR1 and DR2. In a neutral nanocrystal QY_1 can decrease only because of the presence of $\gamma_{NR}\neq 0$, being $\gamma_A = 0$, since Auger recombination is a 3-charges process. In an ionized state also $\gamma_A\neq 0$, and off-states or gray-states can be observed.

When all multi-excitonic Quantum Yields are suppressed by efficient Auger recombination, i.e. $\gamma_A\gg\gamma_R$ in Eq. (3), $QY_m = 0$ for $m > 1$ and the probability of emitting more than one photon per
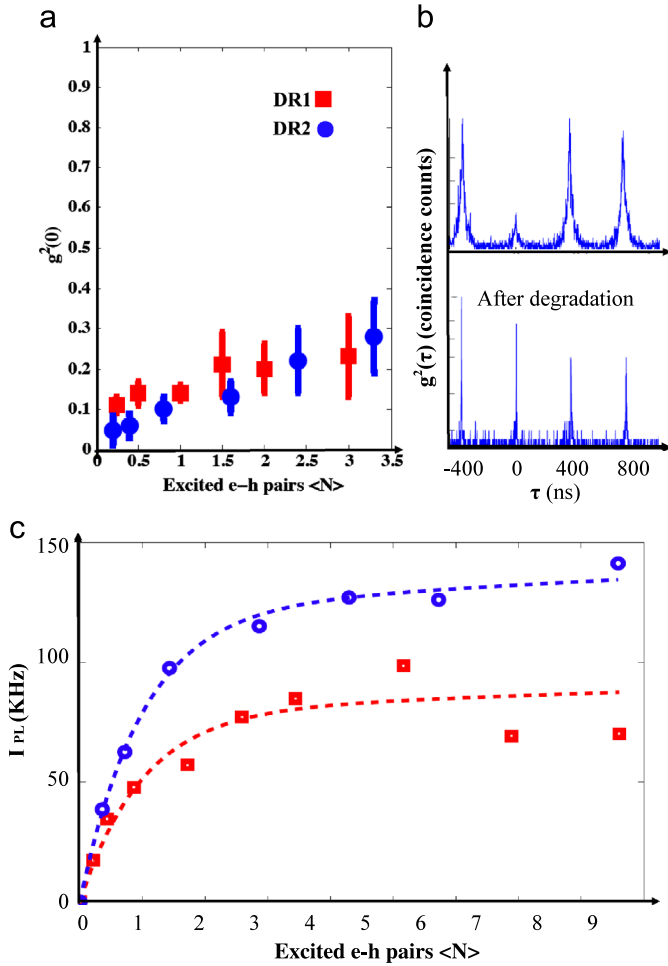
Fig. 2. (a) $g^2(0)$ measurements as a function of the number of electron–hole pairs $\langle N \rangle$ excited by a laser pulse. Despite their different geometrical structures, DR1 and DR2 show similar behaviors. (b) Example of photo-induced degradation of emission properties. Up: $g^2(\tau)$ at low excitation power at the beginning. Down: $g^2(\tau)$ at the same excitation power, but after exposure to high pump fluence. In the picture below, total counts are less, $g^2(0)$ close to 1, and lifetime is decreased. (c) PL counts as a function of $\langle N \rangle$ for DR1 (red squares) and DR2 (blue dots). Points are average values for about 10 single DRs and both curves are fitted by the exponential of Eq. (4). I_{PL} for DR1 is about 60% of DR2, which implies that they have a different single photon Quantum Yield QY_1. (For interpretation of the references to color in this figure caption, the reader is referred to the web version of this article.)

excitation pulse is negligible, so $g^2(0) \simeq 0$. Then Eq. (2) reduces to

$$I_{PL}(P) = I_{sat}(1 - e^{-P/P_{sat}}) \qquad (4)$$

The excitation power P is proportional to $\langle N \rangle$. The saturation power P_{sat} is the power that corresponds to $\langle N \rangle = 1$.

If no Auger effect is present, QY_m is identical for any number m of excited electron–hole pairs, leading to light emission with a Poissonian statistics, and consequently to a $g^2(0)$ equal to 1. Such a 'classical' source of light gives rise to a PL which is proportional to the excitation power.

The saturation of the PL as a function of the excitation power is thus a remarkable signature of single photon emission. One can see in Fig. 2(c) that the measurements performed on the two sets of single DRs satisfy well Eq. (4). This property was used in Fig. 2(a) and (c) to convert the excitation power P into a mean number $\langle N \rangle$ of electron–hole pairs created during each laser pulse, by fitting with Eq. (4) the curve of the PL as a function of P (for single DRs).

These results, both in sample DR1 and DR2, were obtained at rather low excitation power ($\langle N \rangle \lesssim 3$). However, after excitation at high power ($\langle N \rangle \gg 1$), some NCs start to blink more. Single photon

quantum yield QY_1 becomes lower, gray states more frequent and some DRs irreversibly bleach in a state which is slightly above the noise level. In the case some residual emission can still be detected, the result is exemplified in Fig. 2(b): the same NC which exhibited a good single photon emission quality, with a measured QY_1 between 30% and 50%, starts to emit much less. The average lifetime, which was around 30 ns, becomes less than 2 ns (comparable to our system resolution) and, above all, $g^2(0)$ becomes closer to 1 [26].

Summarizing, both DR1 and DR2 have a similar behavior in terms of $g^2(0)$ when a selection of bright and stable NCs is performed, as clearly shown in Fig. 2(a). However, in both cases, some NCs emission degrades over time, especially under high excitation. In single NC measurements it is difficult to see a difference between the 2 samples, since both of them appear to be good single photon source. We will show that this problem can be circumvented by an ensemble measurement, which can demonstrate that the fraction of good single-photon source NCs is very different in the 2 samples, as well as their photo-stability.

The system for NCs ensemble measurements is a home-made confocal microscope, described in Fig. 3(a). It is similar to the one used in single NC $g^2(0)$ measurements, with only one APD detector and an excitation provided by a commercial 405 nm continuous wave diode laser. The beam is enlarged by a telescopic system and then focalized on the sample by means of an air objective with numerical aperture NA=0.85. The objective is embedded into a
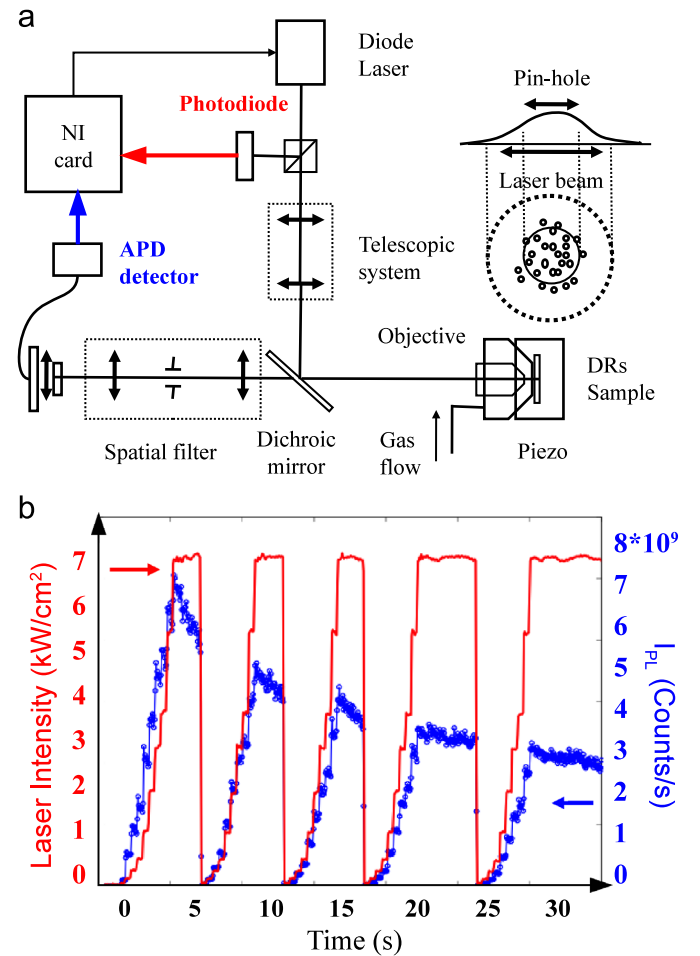

Fig. 3. (a) Experimental apparatus for NCs ensemble measurements. (b) Decay of the PL of DR1 measured with an APD as a function of time under 7 KW/cm² laser excitation. In addition, at selected times $t = 0, 5, 11, 17$ and 24 s, the laser is suddenly turned off and then turned on again to maximum intensity on a time of 3–4 s. The variation of PL during such an event is shown together with the corresponding input laser intensity.

structure that allows us to pump a gas flow of nitrogen directly onto the glass. DRs from a toluene solution at a concentration of 10^{-7} M are drop casted onto a glass cover slip. This density is high enough to collect a good PL signal also at low excitation intensity. By using such a high concentration, which is almost the same as the one used for realizing the TEM images of Fig. 1, a monolayer of about 10^3–10^4 DRs in 1 μm^2 is obtained. The long organic ligands [24] surrounding DRs keep them at a distance of 2–3 nm which is enough to neglect strong interactions like electron tunneling, while longer range dipole interactions like Forster Resonant Energy Transfer (FRET) [28] are limited by the narrow PL spectrum associated with low size dispersion. This is verified by comparing the spectrum of a monolayer of DRs with the same spectrum previously taken in solution.

The sample is mounted on a piezoelectric ceramic. In this way we can perform a scan of the surface in order to check the uniform distribution of emitters. PL is collected from a central region of the laser beam by means of a 100 μm pin-hole, as illustrated in inset of Fig. 3(a). In this way uniform excitation intensity is ensured. PL is transmitted by a dichroic mirror and sent to an APD. The laser power is controlled by a voltage signal provided via computer. An acquisition card allows monitoring the input power, measuring the reflection of the input polarized beam on a beam splitter. The counts detected by the APD are registered by the same card.

The NCs are excited at about 7 kW/cm^2, well above the expected saturation for both the samples under study. With this high excitation power, PL in both cases decays with a time constant of the order of a few tens of seconds, showing a degradation of the emission because of the interactions of photo-excited charges with the environment. At 405 nm the absorption is due to a quasi-continuum of excitonic energy levels, so the number of excited electron–hole pairs is nearly proportional to the volume of the NC. Since the spontaneous decay time of both DR1 and DR2 is almost the same (about 30 ns), the same number of excitons is excited per unit volume and per unit time.

In addition, at some specific times, we suddenly decrease the excitation power down to 25 W/cm^2, well under saturation, and

we scan it back to the value of 7 kW/cm^2 in a few seconds. PL is measured during this scan as can be seen in the inset of Fig. 3(b).

As a result, we have access to the variation of PL as a function of the excitation intensity at different times during the progressive degradation of the DRs. These PL curves, measured with an APD, are shown in Fig. 4.

It can be seen that ensemble PL plots do not show the saturated behavior described by Eq. (4) and found in single NC measurements on a selection of DRs, Fig. 2(c). Moreover, as photobleaching progresses and PL decreases, the shape of the curves goes towards a straight line. As we already mentioned above as a result of Eq. (2), proportionality of PL to excitation power emerges for emitters in which all QY_m become comparable.

Using to the model presented above, we have fitted the PL curves by the function:

$$I_{PL}(P) = \alpha(1 - e^{-P/P_{sat}}) + \beta P. \tag{5}$$

The first term is the exponential variation from Eq. (4), due to the saturation of DRs which are good single photon sources, and the second one gives a linear dependence on the excitation power P. This linear dependence is consistent with the increase in $g^2(0)$ observed in some single DRs, as can be seen in Fig. 2(b) after high photo-excitation, which also makes them low intensity emitters. DRs can be already in this low emitting state after the synthesis because of an intrinsic quality of the sample. Thus, the coefficients α and β in Eq. (5) can be interpreted as two populations of different DRs n_1 and n_2, the first with high single photon Quantum Yield QY_1 and the second with low overall Quantum Yield QY':

$$I_{PL}(P) = n_1 QY_1(1 - e^{-P/P_{sat}}) + n_2 QY' \frac{P}{P_{sat}} \tag{6}$$

A priori this behavior could be assigned to a suppression of Auger rates, as observed in 'giant' NCs [18]. However, since ensemble PL decreases in time over the whole duration of the experiment, as can be seen from the curves taken at various times in Fig. 4, another degradation process must be considered. This process leads to the decrease of the single exciton quantum yield
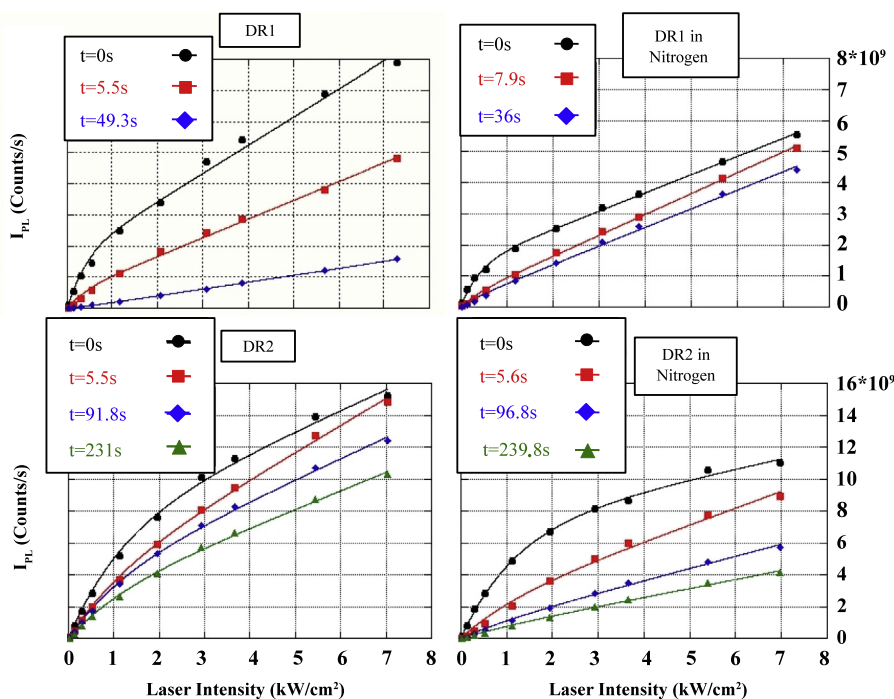

Fig. 4. Dots: Ensemble dot-in-rod PL as a function of laser intensity, at different times during PL degradation induced by continuous 7 kW/cm^2 photo-excitation. Left, in air; right, under a nitrogen flux. Lines: fitting with function in Eq. (5).

Table 1
Summary of fit parameters extracted by ensemble PL measurements in Fig. 4, according to Eq. (5).

Oxygen			Nitrogen		
t (s)	α	β	t (s)	α	β
DR1					
0	1.6	0.9	0	0.54	0.24
5.5	0.44	0.6	7.9	0.12	0.28
49.3	0	0.2	36	0.07	0.25
DR2					
0	6.6	1.3	0	5.8	0.5
5.5	3.3	1.7	5.6	1.6	0.9
91.8	3.4	1.3	96.8	0.5	0.7
231	2.4	1.1	239.8	0.3	0.5

QY_1 which becomes comparable to all the other multi-excitonic recombination yields QY_m. As pointed out above, this can be associated either with a highly ionized state in which all QY_m (included QY_1) scale as γ_R/γ_A or with the opening of non-radiative channels, such as the creation of new defects or dangling bonds at the surface, leading to $QY_m \approx \gamma_R/\gamma_{NR}$. In both cases, overall PL is expected to decrease and single photon emission quantum properties are gradually lost. In the present case the gradual disappearance of the saturation observed in ensemble PL measurements can be assigned to a combination of the degradation processes and of the change in Auger rate γ_A.

Results from the fit are summarized in Table 1.

In most of the cases, an unexpected increase in β coefficient from $t = 0$ s to the second studied time (between 5 and 8 s) is found. This is mainly due to an experimental artifact. In the first few seconds of excitation, the PL decay time can be indeed very short and become comparable to the minimum time in which the laser intensity can be changed and PL counts collected. A priori, this problem could be overcome by a faster electronic control.

An interesting feature of this ensemble method is that it allows to differentiate our two kinds of nanocrystals DR1 and DR2 better than a single emitter study. In Fig. 2(a) DR1 and DR2 appeared to have a similar performance as single photon sources, whereas Fig. 4 (left panels) shows clearly that they have very different behaviors. DR1 loose any saturation component after few seconds, while DR2 at $t = 231$ s have a weight of the exponential which is still more than $\frac{1}{3}$ of what it was at $t = 0$ s.

Furthermore this method allows to study the different behaviour of the nanocrystals in an atmosphere of pure nitrogen, as can be seen in Fig. 4 (right panels). In both samples at $t = 0$ s PL mean intensity is lower when the samples are excited under nitrogen atmosphere. In the case of DR1, the saturation component disappears very rapidly both under nitrogen and standard air conditions, while nitrogen seems to slow down in some way a degradation process affecting the linear PL component. In the case of DR2, on the other hand, the presence of oxygen in the atmosphere surrounding the nanocrystals is found to be very important for preserving the single photon character of NCs. The role of the oxygen in preserving both photon statistics and photo-stability, at least under conditions of high excitation, can be interpreted, as suggested by Müller [23], in terms of controlling the NC state of charge. The tendency to hole trapping under photo-excitation, and so the prevalence of negative charged NCs (also called trion), has been recently demonstrated in spherical NCs of CdSe/CdS [27]. Thus, in standard atmospheric conditions, a transfer of electrons to oxygen is possible, which can lead to neutralization of charged, non emissive DRs.

In conclusion we have described a new ensemble-based experimental method to study the quality of a sample of NCs as single photon source and its photo-stability under condition of high excitation and in the presence or absence of oxygen. We demonstrated the interest of the method by identifying significant differences between two samples of DR with similar performances as single photon sources when single isolated NCs were observed. This method can easily be applied to any artificial nano-structures that need to be characterized as single photon source. It allows a fast discrimination between different kinds of samples, or different synthesis of the same sample, to test the quality of the conservation of a sample, or its interaction with a substrate.

Acknowledgments

References

[1] C.B. Murray, D.J. Norris, M.G. Bawendi, Journal of American Chemical Society 115 (19) (1993) 8706, http://dx.doi.org/10.1021/ja00072a025.
[2] A.P. Alivisatos, Science 271 (5251) (1996) 933, http://dx.doi.org/10.1126/science.271.5251.933.
[3] M.A. Hines, P. Guyot-Sionnest, Journal of Physical Chemistry 100 (1996) 468.
[4] P. Michler, A. Imamoglu, M.D. Mason, P.J. Carson, G.F. Strouse, S.K. Buratto, Nature 406 (2000) 968.
[5] M. De Vittorio, F. Pisanello, L. Martiradonna, A. Qualtieri, T. Stomeo, A. Bramati, R. Cingolani, Opto-electronic Review 18 (1) (2010) 1.
[6] D.I. Chepic, Al.L. Efros, A.I. Ekimov, M.G. Ivanov, V.A. Kharchenko, I.A. Kudriavtsev, T.V. Yazeva, Journal of Luminescence 47 (1990) 113.
[7] M. Kuno, D.P. Fromm, H.F. Hamann, A. Gallagher, D.J. Nesbitt, Journal of Chemical Physics 112 (2000) 3117.
[8] Al.L. Efros, M. Rosen, Physical Review Letters 78 (1997) 1110.
[9] C. Galland, Y. Ghosh, A. Steinbruck, M. Sykora, J.A. Hollingsworth, V.I. Klimov, H. Htoon, Nature 479 (2011) 203.
[10] Robert M. Dickson, Andrew B. Cubitt, Roger Y. Tsien, W.E. Moerner, Nature 388 (1997) 355.
[11] P. Spinicelli, S. Buil, X. Quélin, B. Mahler, B. Dubertret, J.-P. Hermier, Physical Review Letters 102 (2009) 136801.
[12] L. Xu, X. Huang, J. Zhu, H. Chen, K. Chen, Journal of Material Science 35 (2000) 1375.
[13] X. Wang, X. Ren, K. Kahen, M.A. Hahn, M. Rajeswaran, S. Maccagnano-Zacher, J. Silcox, G.E. Cragg, A.L. Efros, T.D. Krauss, Nature 459 (2009) 686.
[14] M. Zavelani-Rossi, M. Lupo, F. Tassone, L. Manna, L. Lanzani, Nano Letters 10 (2010) 3142.
[15] F. Pisanello, G. Leménager, L. Martiradonna, L. Carbone, S. Vezzoli, P. Desfonds, P.D. Cozzoli, J.-P. Hermier, E. Giacobino, R. Cingolani, M. De Vittorio, A. Bramati, Advanced Materials (2013), doi: http://dx.doi.org/10.1002/adma.201203171.
[16] Y. Chen, J. Vela, H. Htoon, J.L. Casson, D.J. Werder, D.A. Bussian, V.I. Klimov, J.A. Hollingsworth, Journal of American Chemical Society 130 (2008) 5026.
[17] B. Mahler, P. Spinicelli, S. Buil, X. Quelin, J.P. Hermier, B. Dubertret, Nature Materials 7 (2008) 659.
[18] Y.-S. Park, A.V. Malko, J. Vela, Y. Chen, Y. Ghosh, F. Garcia-Santamaria, J.A. Hollingsworth, V.I. Klimov, H. Htoon, Physical Review Letters 106 (2011) 187401.
[19] W. Qin, P. Guyot-Sionnest, ACS Nano 6 (2012) 9125.
[20] A. Biebricher, M. Sauer, P. Tinnefeld, Journal of Physical Chemistry B 110 (2006) 5174.
[21] L. Hartmann, A. Kumar, M. Welker, A. Fiore, C. Julien-Rabant, M. Gromova, M. Bardet, P. Reiss, P.N.W. Baxter, F. Chandezon, R.B. Pansu, ACS Nano 6 (2012) 9033.
[22] W.G.J.H.M. van Sark, P.L.T.M. Frederix, A.A. Bol, H.C. Gerritsen, A. Meijerink, ChemPhysChem 3 (2002) 871.
[23] J. Muller, J.M. Lupton, A.L. Rogach, J. Feldmann, D.V. Talapin, H. Weller, Applied Physics Letters 85 (3) (2004) 381.
[24] L. Carbone, C. Nobile, M. De Giorgi, F. Della Sala, G. Morello, P. Pompa, M. Hytch, E. Snoeck, A. Fiore, I.R. Franchini, M. Nadasan, A.F. Silvestre, L. Chiodo, S. Kudera, R. Cingolani, R. Krahne, L. Manna, Nano Letters 7 (2007) 2942.
[25] G. Nair, J. Zhao, M.G. Bawendi, Nano Letters 11 (2011) 1136.
[26] X. Xu, T. Yamada, A. Otomo, Applied Physics B 94 (2009) 577.
[27] C. Galland, Y. Ghosh, A. Steinbruck, J. Hollingsworth, H. Htoon, V. Klimov, Nature Communications 3 (2012) 908.
[28] T. Forster, Naturwissenschaften 33 (1946) 166.